

Relationships between of Sediment Concentrations from ^{10}Be Analysis and Morphometric Aspect in Sangun Catchment Area, Fukuoka Prefecture, Japan

Hendra Pachri¹, Yasuhiro Mitani¹, Hiro Ikemi¹, Ryunosuke Nakanishi¹ and Yoko Saito-Kokubu²

1. Dept. of Civil Engineering, Faculty of Engineering, Kyushu University, Japan

2. Tono Geoscience Center, Japan Atomic Energy Agency (JAEA), 959-31, Jorinji, Izumi, Toki, Gifu 509-5102, Japan

Abstract: Recently, the contributions of slope failures have been difficult to quantify over the time scales of the sediment concentrations in Sangun catchment area, Fukuoka Prefecture. Therefore, to clarify the sources of the sediment mixing in the catchment is important and becomes considering in the future that related the slope failures occurrence. This paper describes how cosmogenic nuclide methods have provided information about the geomorphic process by utilizing ^{10}Be (half-life = 1.5 ma), measuring the $^{10}\text{Be}/^9\text{Be}$ ratio, and quantifying ^{10}Be concentration. The sampled sediments were derived from throughout a drainage basin. To measure the $^{10}\text{Be}/^9\text{Be}$ ratios in the sediments, quartz minerals were collected from the sediment and then Be was extracted from the quartz. The $^{10}\text{Be}/^9\text{Be}$ ratios were measured by AMS. We assume that the cosmogenic nuclide concentrations stored in the sediment of a river can increase or decrease, depending on the amount of mixing of sediments during transport through the fluvial system. As results, the ^{10}Be concentrations have been calculated to determine the short term sediment mixing rate in the catchment area. Therefore, the relationship between the morphometrics of the drainage basin, the sediment concentration by ^{10}Be analysis and the contribution of landslides to landscape changes over timescales of several years have been investigated in Sangun catchment area.

Key words: Slope failures, ^{10}Be concentrations, morphometric, river sediment.

1. Introduction

Wang [1], in a summary of works by other authors, reported that in mountainous regions around the world landslides and debris flows are a source of severe natural disasters and societal hazard. Analyzing the relationship between landslides and the various factors causing landslides not only provides an insight to understand landslide mechanisms, but can also form a basis for predicting future landslides and assessing landslide hazard. In areas with similar geotechnical conditions, researchers generally make two fundamental assumptions. Landslides will occur in the same geological, geomorphological, hydrogeological and climatic conditions as in the past [2, 3]. On the other hand, the properties and types of landslides will

also be the same.

Therefore, the study of the mechanisms and properties of past landslide is a valuable reference for assessing the future landslide hazard in adjacent or geotechnically similar areas. However, there is little field data to either evaluate the validity of the proposed slope stability calculation or to quantify any of the sediment rates. It has frequently been suggested that gravity-driven soil creep is an important transport process for many soil-mantled hillslopes. Gilbert (1877, 1909) in [4] proposed that the rate of soil creep is proportional to the slope gradient and that a slope may achieve a condition of dynamic equilibrium. On such slopes both the soil thickness and the rate of soil production by rock weathering are uniform and the soil creep flux increases with distance from the top of the slope. It then follows [4] that the slope must steepen with distance from the divide; i.e., the slope profile

Corresponding author: Hendra Pachri, Ph.D. candidate, research fields: engineering geology, slope failure assessment, and sediment disaster.

must be convex upward to provide the necessary transport capacity.

This hypothesis is the basis for many models that use slope-dependent soil transport laws to investigate the evolution of soil-mantled hillslopes. Currently, fine sediment flux prediction at the watershed scale is limited by the precision of erosion rate estimates for the many potential sources distributed throughout a landscape, as well as our understanding of the connectivity of sediment pathways during transport [5]. Cosmogenic nuclide surface exposure dating has generated important new insights into landscape evolution and surface process rates. Nishiizume et al. [6] attempted to sketch a general model with new in situ ^{10}Be and ^{26}Al measurements in different types of geomorphic situations. Their conclusion was that cosmogenic nuclides are not simply a single surface exposure dating method, but rather a set of tools to study a geomorphic processes on timescales that are truly appropriate for development of most landscapes.

Application for cosmogenic ^{10}Be proceeded in quartz of river sediment could follow that serve as a tool as powerful as the in situ produced cosmogenic nuclides to derive erosion rates and soil residence times from individual soil surface samples or detrital river sediment [7]. River sediments are eroded at different rates in different source areas (i.e. different sub-catchments) and therefore inherit different nuclide concentrations. The mixing of grains through hillslope and fluvial transport processes homogenizes nuclides in the downstream sediment load. Therefore, a handful of sediment collected from a river bed can lead to a profoundly new understanding of the rates of landscape change [8]. Recently, several research groups have begun to measure the abundance of nuclides in sediments with the goal of estimating basin-scale rates of denudation [9].

We assume that storage in a river can increase or decrease the cosmogenic nuclide concentrations in sediment, depending on the amount of mixing of sediments during transport through the fluvial system.

In a system with significant sediment storage, the sediment flux time can be examined using a pair of in situ produced cosmogenic radionuclides with appropriately differing half-lives. Here, we calculate the in situ cosmogenic nuclide concentration in alluvial sediment to further the understanding of the sources and the process of sediment mixing for an area of 1.676 km². We compare data on the concentration of sediment mixing from four sites along the main stream of the Sangun river catchment and from four of its smaller tributaries with slope failure data, as well as investigating the morphometric and geologic controls on low-frequency, high-magnitude sediment discharges. The particular geomorphic setting of the catchment additionally allows evaluation of the effects of different processes (slope failures) on ^{10}Be concentrations in alluvial sediment. In this paper, we provide the important relationships between the cosmogenic nuclides and several geomorphic parameters that relate to sediment supply through slope failure events on cosmogenic nuclide concentrations in rivers.

2. Study Area

2.1 Geographic Settings

The catchment is located in a mountainous region in northern Kyushu, Japan, the Sangun mountain massif (Fig. 1). The mountain catchment is a hazardous area for sediment disasters. In this area, a large number of shallow slope collapses and subsequent debris flows have occurred due to heavy rain. All the alluvial sediment and hillslope samples were from channels on the western slopes of the Sangun Mountain catchment. The hillslopes at high elevations in the basin have two zones, west and south. Central towards the western part is a residential zone, where there has been a high probability of slope failure occurring in the past.

2.2 Geology of Sangun Mountains

The geology consists mainly of Mesozoic granitic

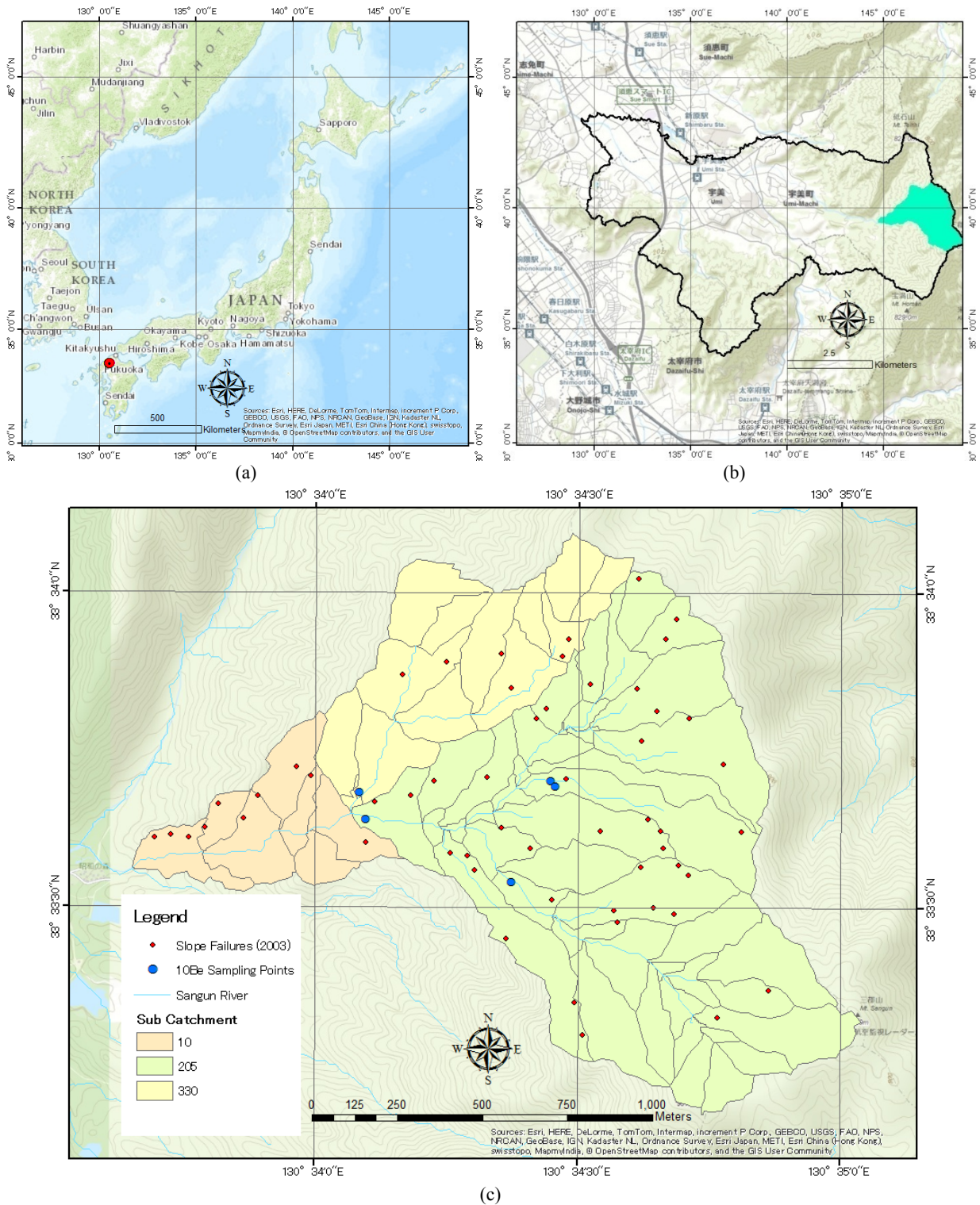


Fig. 1 Sangun basin boundary (b) and inventory of slope failure map and small catchment at upstream part are selected for ^{10}Be investigations (c).

rocks. Paleozoic and Mesozoic metamorphic rocks can also be observed on some valley slopes as roof pendants, but they are limited [10]. Most of soil is

produced from granite rock weathering. The soil depth ranged from 0.51 m to 1 m has the largest area of soil distribution [26].

3. Datasets and Methods

3.1 Field Investigation

A sample of sediment collected at the outlet of a catchment is assumed to be an aggregate of grains that originate from all of the different regions in the upstream area (Fig. 1). In this study, sediments were collected across the width of the river channel and hillslopes. Samples were collected in November 2014. Locations were determined by using a hand-held Garmin GPS (Table 2). We also sampled one hillslope area, assumed to be the source of sediments from the slope failure aspect. We collected a total of five samples for ^{10}Be analysis: four samples were taken from alluvial sediments within the channel network and were used to analyze the effect of sediment mixing, and one sample was collected from the hillslope, yielding information about the background slope failure on hillslopes.

To investigate the ^{10}Be concentration related to the mixing of sediment, samples were taken from the upstream of Sangun main channel. Two samples were collected from the outlet of the slope failure catchment as it hosts two separate channels. The location of the samples and their relationship to the stream's long-profile are shown in Fig. 3.

3.2 Extraction of Basin Morphometrics

A digital elevation model (DEM) of the Sangun basin was assembled from 5-meter airborne laser survey data (LiDAR data) obtained from the local governments in Japan. The Sangun sub-basins were rectified and delineated in ArcGIS 10.1 by using the hydrology tool. Morphometric properties of the basin were extracted and calculated in ArcMap 10.1.

Channel longitudinal profiles and channel slope-basin area analysis were generated.

3.3 Slope Failures in the Catchment

In this study, a slope failures location map was prepared based on the previous researches conducted in the area and aerial photographs (Fig. 1). In addition, field work was carried out to map recent landslides. The instability factors were chosen based on the abovementioned studies carried out in the study area, the bibliographical review and from field investigations.

3.4 Concentration in ^{10}Be Analysis

Samples were treated to isolate 20 to 60 grams of pure quartz from samples. The experimental work required for the measurements of in situ produced nuclides with quartz rich minerals has some chemical aspects [11]. The three major experimental steps classified are: (1) separation of purified quartz mineral; (2) BeO preparation for AMS targets; and (3) measurement of $^{10}\text{Be}/^9\text{Be}$ ratio by AMS. For ^{10}Be analysis, the most important characteristic is the ability to prepare a sample that is free of atmospherically produced ^{10}Be [12]. Quartz has been shown to be useful because it is resistant to weathering and alteration and can be effectively cleaned of meteoric ^{10}Be by HF etching [13-15]. The procedures of (1) and (2) are following the method of Kohl and Nishiizumi [13].

(1) Separation of purified quartz mineral

As a first step, the river sediment samples were dried in an oven. The river sediments were sieved to 0.25-1 mm size fractions for analysis. Eliminating easily dissolved minerals without losing any quartz is important in the experiment, therefore HCl was used as the first chemical treatment [15]. The second process

Table 1 Distribution of slope failures as sediment prediction source in the upper part of Sangun catchment area.

No	Sample ID	Number of slope failures (unit) (a)	Drainage area (m^2) (b)	Ratio a/b (%)	Slope angle mean ($^\circ$)
1	93R	2	84,573.58	21.01	38.1
2	93S	2	84,573.58	21.01	38.1
3	201	10	440,455.54	20.17	39.2
4	205	25	1,148,014.56	20.89	36.2
5	330	6	315,142.07	16.91	37.7

was an HF leaching which is the most effective method to eliminate unwanted silicate minerals and to maximize the purity and yield of the final quartz. Furthermore, other minerals except for the quartz particles were hand-picked out.

(2) BeO preparation for AMS targets

The procedures are as follows: (a) addition of carrier; (b) dissolution of quartz; (c) anion exchange; (d) cation exchange; (e) precipitation cleaning; (f) oxidation; and (g) BeO pressed to target. The process of (a) consists of taking about 20 g pure quartz, adding ^{10}Be carrier (0.3 mg).

In the procedure (b), the quartz was dissolved by HNO_3 , HClO_4 and HF. After that, the Be was separated from other elements through anion exchange (DOWEX 1-X8, 100-200 mesh) and then through cation exchange (DOWEX 50W-X8, 100-200 mesh) $\text{Be}(\text{OH})_2$ was precipitated from the separated solution with diluted ammonia and was converted to BeO by heating at 800°C for about 10 minutes. Then pressed into AMS target holder being mixed with Nb powder.

(3) Measurement of $^{10}\text{Be}/^9\text{Be}$ ratio performed

Measurements were performed by the JAEA-AMS-TONO facility at the Tono Geoscience Center of the JAEA [16]. The $^{10}\text{Be}/^9\text{Be}$ ratio was calibrated against the standards (01-5-1) supplied from University of California [16, 17].

3.5 ^{10}Be Concentration and Production Rates Calculations

The ^{10}Be concentration calculations were performed following Balco et al. (2008) by converting Be isotope ratio measurements to nuclide concentrations in quartz [25]. The ^{10}Be concentration in quartz is the quantity needed to calculate a production rate. Production rate calculations were performed following Balco et al. (2008) in Savi et al. (2013) using the CRONUS EARTH calculator (ver. 2.2; <http://hess.ess.washington.edu/>) [19]. Topographic aspects such as latitude, longitude and the mean elevation of sites in the catchment were determined

from a digital elevation model (DEM) with 5 m resolution.

4. Results

4.1 Relationship of Drainage Area and Slope Angle in the Catchment Area

Fig. 2 shows the relationships between the drainage area and slope angle at the upper stream in the Sangun catchment. We divided the small catchment into three parts, indicated in the figure by different colors. Black circles show the right part of the upper stream (catch. 205 in Fig. 1), brown triangles show the downstream part of the catchment (catch. 201 in Fig. 1), and blue rectangles show the left part of the upper stream (catch. 330 in Fig. 1). The distribution of the slope angle shows the majority in the range of 25° to 45° for the drainage area of less than $9 \times 10^4 \text{ m}^2$.

4.2 Longitudinal Profiles

Fig. 3 shows the sampling location, relating the stream and catchment topographic profiles of the upstream part of the Sangun catchment. The ridgeline elevations are shown as red (330), gray (205 and 201), and green (both 93R and 93S, as inlets to 205) lines.

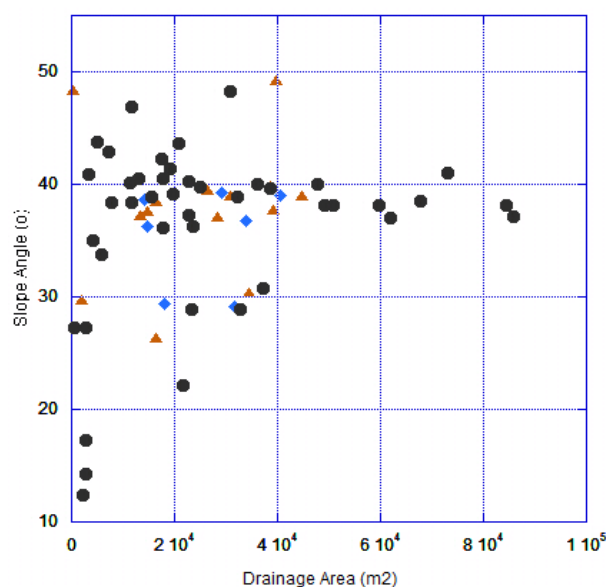


Fig. 2 Slope angle ($^\circ$) versus drainage area (m^2) on the upper stream in the Sangun catchment area.

Relationships between of Sediment Concentrations from ^{10}Be Analysis and Morphometric Aspect in Sangun Catchment Area, Fukuoka Prefecture, Japan

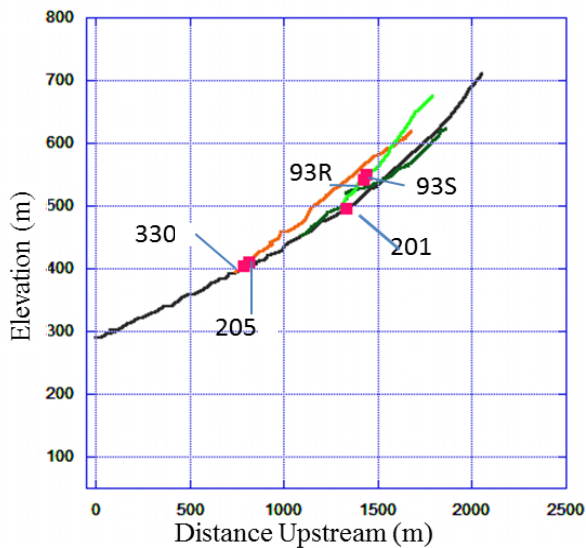


Fig. 3 Elevation (m) versus upstream distance (m) on the upper stream in the Sangun catchment area.

In the figure, we divide the river flow into two parts as the source of sediment materials.

Point 330 presents the first river flow, and points 205, 201, 93R, and 93S represent the second river flow. The elevations and distance upstream are indicated.

4.3 Slope Failure in Sangun Catchment Area

Mountainous catchments, especially in the Sangun region, are hazardous areas for sediment disasters. On July 18-19, 2003, a short duration, high-intensity rainfall event impacted the city of Sangun area in Fukuoka Prefecture, Japan (Fig. 1). The rainfall triggered many landslides and debris flows [18]. The slope failure and resultant debris flow in the Sangun area was the largest and most damaging of these disasters. A moderate size, 1-8 m deep debris

avalanche triggered the debris flow about 0.5 km at the upslope of where the casualties occurred.

The rainfall intensity that struck the village of Sangun area was estimated as about 315 mm/day, and the density of slope failure was estimated about 48 points/km². Based on the aerial map and field investigation, a number slope failure in the study area was 55 points. Table 1 shows the number of slope failures along the river catchment that are assumed to be the source of sediment to the sampling points. The number of slope failures in the 330 catchment represents the first part of the small catchment area, and at 205 represents the second part. In the table, the number of slope failures at site 205 is higher than at 330.

4.4 ^{10}Be Concentrations in River Sediments

Table 2 shows that the ^{10}Be concentrations in river sediments vary geographically over the 330 and 205 catchments of the sub-catchment area. These results of the ^{10}Be concentration allow the identification of two groups, the 330 and the offers (the 205 group). The 330 site has the highest concentration, which implies that it has experienced the lowest of total number of slope failures. The 205 samples have the lowest ^{10}Be concentration, implying the highest of number of slope failures and assumed to be derived from the landslides and debris flow catchment. However, the 93S sample is source sediment towards the 205 site and has a higher ^{10}Be concentration than the other points in the 205 group.

Table 2 ^{10}Be concentrations of rivers sediments in the upper part of Sangun catchment area.

No	Sample ID	North	East	Altitude (m)	Ratio of $^{10}\text{Be}/\rho\text{Be}$ (10^{-13})	1σ error (10^{-13})	^{10}Be concentrations (10^4 atoms/g)	1σ error (10^6 atoms/g)	^{10}Be production rate (atom/g/yr)	1σ error (atom/g/y)
1	93R	-39540.8405	62369.975	552.433	0.97	0.18	3.34	0.79	6.06	0.22
2	93S	-39540.8405	62369.975	556.400	1.10	0.13	5.48	0.92	6.08	0.22
3	201	-39656.363	62072.8883	485.579	0.89	0.35	3.11	0.51	5.75	0.21
4	205	-40086.9805	62259.3318	398.859	1.01	0.15	4.01	0.80	5.35	0.20
5	330	-40102.8991	62338.5854	417.160	2.16	0.1	8.73	1.85	5.45	0.20

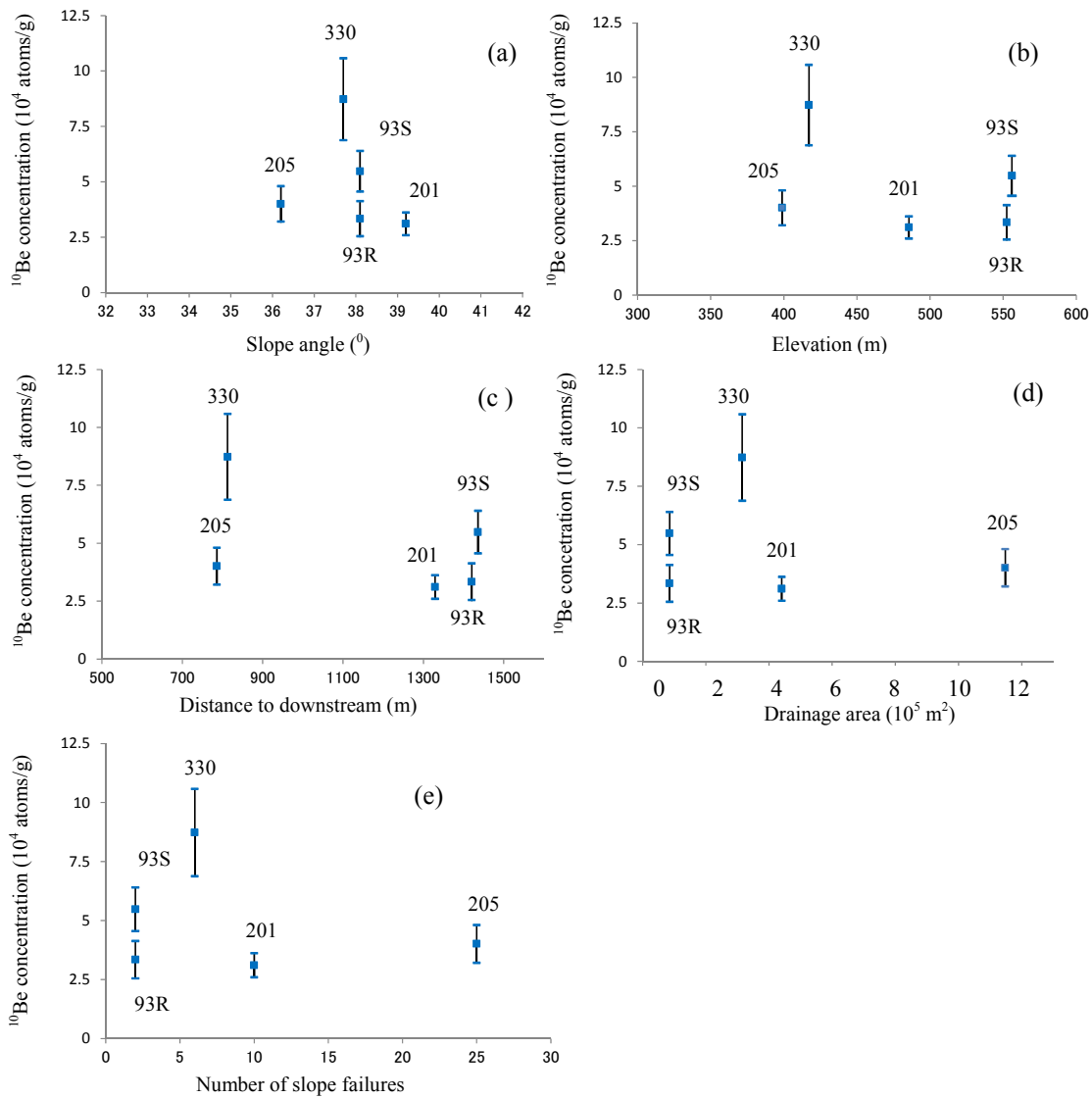


Fig. 4 Relationships between ^{10}Be concentrations in river sediments and geomorphic parameters (see text for details).

5. Discussion

5.1 ^{10}Be Concentrations in an Upper Stream of Sangun Catchment

Disparities in the ^{10}Be concentration values of two groups in river sediment indicate different exposure histories experienced by the different material sources and processes. In recent years, observation of the ^{10}Be concentration relationship has been widely used to derive geomorphologic processes in a catchment regarding the influence of landslide processes in mountainous environments [19-21]. In this study, we

present a new data set of ^{10}Be concentrations in river sediments sampled along the Sangun river and one sample on the hillslopes. We interpret the ^{10}Be concentrations as being impacted by sediments derived from hillslope processes along the Sangun river. We find that ^{10}Be concentrations differ significantly between the 330 and 205 sites (Table 2). Both the 330 and 205 sites will provide the hillslopes processes. The relationships between the ^{10}Be concentrations and the distribution of slope failure in the catchment suggest the influence of mass movement processes in the river sediment storage.

Fig. 4e shows an inverse relationship between the number of slope failures and ^{10}Be concentrations for both the 330 and 205 sites. The percentage of ratio of the number of slope failures and drainage area in the 330 and 205 sites indicates how much the responsible a slope failure quantity in the sites. The 330 site shows lower values than the 205 sites. In the short term, sediment materials may not be affected by slope failures. Sediment materials may also be preferentially produced by chemical weathering in the long term.

The higher ^{10}Be concentration in the samples can be explained by a combination of a rock weathering, preferential production at high elevations, mass movement process by long hillslopes transport. The gravel may correspond to the typical class size produced by fraction at high elevation, where the ^{10}Be production rate is high [22]. At 330 site, the ^{10}Be production rate is 5.45 ± 0.2 atom/g/yr. Alternatively, we have found a relationship between weathering grade and ^{10}Be concentration by examining the silica content in the river water. The ^{10}Be concentration at the 330 site has a larger of weathering grade than the 205 site. Borrelli et al. (2015) reported that in regions where crystalline rocks are widespread, slope stability and morphodynamic evolution of the slope are strongly related to both the thickness of weathering profiles and the intensity of rock weathering [23]. It is assumed that regolith is produced by long hillslopes transport, the imperceptibly slow, steady, downward movement of slope forming soil or rock. In the long term, this process is continuous, where the shear stress continuously exceeds the strength of the rock granite. In the slope movement, these landslides are of the soil creep type [24]. Field observations of soil creep are indicated by curved tree trunks, retaining walls, and small soil ripples. Moreover, in the 205 catchment boundary, the ^{10}Be concentration shows similar values except at the 93S site. The 93S site is representative of the hillslopes sample. It has a higher ^{10}Be concentration than the 93R site (Table 2).

This phenomenon may correspond to a typical grain

size produced by physical weathering at high elevation, or by the breaking of larger pebbles produced at high elevations during long hillslopes transport. At the 205 site boundary, we assume that both the type of landslide in 2003 and soil creep in the long term are affecting the river sediment mixing reflected in the ^{10}Be concentration.

5.2 Catchment Morphometry Controls on Sediment Mixing

We explored the correlations between the ^{10}Be concentrations and several geomorphic parameters, as illustrated by Fig. 4. There is no relationship between these concentrations and elevation, except at the 205 tributary which has a lower ^{10}Be concentration with increased elevation than the 330 tributaries (Fig. 4b). Also, no clear correlation is seen with the slope angle (Fig. 4a). The 330 site shows higher ^{10}Be concentrations than the 205 site. Moreover, the 205 catchments (205, 201, and 93R) show the ^{10}Be concentrations almost same with the slope angle increases (Fig. 4a). Furthermore, there is no clear relationship between the proportion of steep area and the concentration of ^{10}Be [25].

No clear relationships appear on the graphs plotting the ^{10}Be concentrations against the distance to downstream (Fig. 4c). The 330 site shows a higher ^{10}Be concentration than the 205 site with increased distance to downstream. However, in the 205 catchments, the ^{10}Be concentrations decrease as the distance to downstream increases. This graph is the same pattern as for the elevation parameter. Fig. 2 shows both sites the 330 and 205 of the outlets of each small catchment. This means that the accumulation of sediment mixing is present at the site. The length of the river tributary at site 330 is shorter than the 205 tributaries. This makes it clear that the ^{10}Be concentrations are not affected by the length of the river in the catchment.

The larger drainage area in the catchment does not seem to affect the ^{10}Be concentrations, where data

exist (Fig. 4d). The 330 site has larger ^{10}Be concentrations than the 205 site although the drainage area of the 330 site is smaller than the 205 site. This makes it clear that the largest drainage area has no linear relationship with the amount of sediment produced, and it may be influenced by the weathering of rock in the long term. Moreover, in the 205 catchment, the ^{10}Be concentration increases as the drainage area increases except at the 93S site. The 205 site presents the accumulation of sediment delivery from the upstream via the 93R and 201 tributaries. This suggests that the sediment deposited at the 93S site is delivered from the top of the mountain and may not be directed to flow down the river. M. Schaller et al. (2001) presented that hillslope transport processes in middle Europe are dominated by mechanisms such as slow creep and surface wash and that landsliding does not play an important role [26].

6. Conclusions

We have shown here that in the slope failure activity, insufficient sediment mixing can occur to derive sub-basin denudation rates using ^{10}Be concentrations. Therefore, creep processes are the dominant mechanisms of sediment discharge rather than slope failure processes in the Sangun catchment. The difference between the rates of ^{10}Be concentrations suggests that stored sediment is currently being eroded from the upper catchment by creep and slope failure process.

Graps plotting the correlations between the ^{10}Be concentration and several geomorphic parameters show no apparent relationships. In this study, the ^{10}Be concentrations have provided a relationship with sediment disaster that was not affected by slope failures in the 2003. This suggests that application of ^{10}Be concentrations can be considered in the river basin management at Sangun catchment area.

Acknowledgments

The authors would like to thank the Indonesian

Government, Directorate General of Higher Education for its DIKTI Scholarship and we also thank Prof. Dr. Takaichi Kuroki of Fukuoka University for field work. This work was supported by JSPS KAKENHI Grant Number 25350429. This work was performed under the Shared Use Program of JAEA Facilities.

References

- [1] Wang, C., Esaki, T., Xie, M., and Qiu, C. 2006. "Landslide and Debris-Flow Hazard Analysis and Prediction Using GIS in Minamata-Hougawachi Area, Japan." *Environ. Geol.* 51: 91-102.
- [2] Aleotti, P., and Chowdhury, R. 1999. "Landslide Hazard Assessment: Summary Review and New Perspectives." *Bull. Eng. Geol. Environ.* 58: 21-44.
- [3] Hutchinson, J. N. 1995. "Landslide Hazard Assessment." Keynote paper. In: Bell, D. H. (ed.) *Landslides, Proceedings of 6th International Symposium on Landslides*. Christchurch, New Zealand, Vol. 1., Balkema, Rotterdam, 1805-41.
- [4] McKean, J. A., Dietrich, W. E., Finkel, R. C., Southon, J. R., and Caffee, M. W. 1993. "Quantification of Soil Production and Downslope Creep Rates from Cosmogenic ^{10}Be Accumulations on a Hillslope Profile." *Geology* 21: 343-6.
- [5] Stout, J. C. 2012. *Identifying and Quantifying Sediment Source and Sinks in the Root River, Southeastern Minnesota*. M.Sc. thesis, Utah State University.
- [6] Nishiizumi, K. et al. 1993. "Role of in Situ Cosmogenic Nuclides ^{10}Be and ^{26}Al in the Study of Diverse Geomorphic Processes." *Earth Surface Processes and Landforms* 18 (5): 407-25.
- [7] Willenbring, J. K., and Blanckenburg, F. V. 2010. "Meteoritic Cosmogenic Beryllium-10 Adsorbed to River Sediment and Soil." *Applications for Earth-Surface Dynamics. Earth-Science Review* 98: 105-22.
- [8] Von Blanckenburg, F. 2005. "The Control Mechanisms of Erosion and Weathering at Basin Scale from Cosmogenic Nuclides in River Sediment." *Earth and Planetary Science Letters* 237: 462-79.
- [9] Bierman, P. R. et al. 1998. "Erosion, Weathering, and Sedimentation." In: Kendall, C., and McDonnell, J. J. (eds.) *Isotope Tracers in Catchment Hydrology*. Elsevier Science. Chapter 19.
- [10] Association of Sabo DAM, Fukuoka Prefecture. 2014. Geological map of Fukuoka Prefecture, scale 1:150,000.
- [11] Altmaier, M., Klas, W., and Hergers, U. 2001. "Surface Exposure Dating by In-Situ Produced Cosmogenic Nuclides: Chemical Mineral Separation of Purified Quartz." *Radiochim. Acta* 89: 779-82.

- [12] Bierman, P. R. 1994. "Using in Situ Cosmogenic Isotopes to Estimate Rates of Landscape Evolution: A Review from the Geomorphic Perspective." *Journal of Geophysical Research* 99: 13,885-96.
- [13] Nishiizumi, K. et al. 1991. "Cosmic Ray Produced Be-10 and Al-26 in Antarctic Rock Exposure and Erosion History." *Earth and Planetary Science Letters* 104: 440-54.
- [14] Brown, E. T. et al. 1991. "Examination of Surface Exposure Ages of Antarctic Moraines Using in Situ Produced ^{10}Be and ^{26}Al ." *Geochimica et Cosmochimica Acta* 55: 2,269-83.
- [15] Kohl, C. P., and Nishiizumi, K. 1992. "Chemical Isolation of Quartz for Measurement of In-Situ-Produced Cosmogenic Nuclides." *Geochimica et Cosmochimica Acta* 56: 3,583-7.
- [16] Matsubara, A., Saito-Kokubu, Y., Nishizawa, A., Miyake, M., Ishimaru, T., and Umeda, K. 2014. "Quaternary Geochronology Using Accelerator Mass Spectrometer (AMS): Current Status of the AMS System at the Tono Geoscience Center." *Geochronology*, edited by J. van Mourik, 3-30, InTech.
- [17] Nishiizumi, K., Imamura, M., Caffee, M. W., Southon, J. R., Finkel, R. C. et al. 2007. "Absolute Calibration of ^{10}Be AMS standards." *Nuclear Instruments and Methods in Physics Research Section B: Beam Interactions with Materials and Atoms* 258: 403-13.
- [18] Hanamura, Y. et al. 2004. "Heavy Rain Disaster in Kyushu Area on July 2003." *Japan Society of Engineering Geology* 25: 30-1.
- [19] Savi, S., Norton, K. P., Picotti, V., Brardinoni, F., Akcar, N., Kubik, P. W., Delunel, R., and Schlunegger, F. 2013. "Effects of Sediment Mixing on ^{10}Be Concentrations in the Zielbach Catchment, Central-Eastern Italian Alps." *Quaternary Geochronology*. DOI. 0.1016/j.quageo.2013.01.006.
- [20] Belmont, P., Pazzaglia, F. J., and Gosse, J. C. 2007. "Cosmogenic ^{10}Be as a Tracer for Hillslope and Channel Sediment Dynamic in the Clearwater River, Western Washington State." *Earth Planet. Sci. Lett.* 264 (1): 123-35.
- [21] Binnie, S. A., Phillips, W. M., Summerfield, M. A., and Fifield, L. K. 2006. "Sediment Mixing and Basin-Wide Cosmogenic Nuclide Analysis in Rapidly Eroding Mountainous Environments." *Quaternary Geochronology* 1(1): 4-14.
- [22] Carretie, S., Regard, V., Vassallo, R., Aguilar, G., Martinod, J., Riquelme, R., Christophoul, F., Charrier, R., Gayer, E., Farias, M., Audin, L., and Lagane, C. 2015. "Differences in ^{10}Be Concentrations between River Sand, Gravel and Pebbles along the Western Side of the Central Andes." *Quaternary Geochronology* 27: 33-51.
- [23] Borelli, L., Coniglio, S., Critelli, S., La Barbera, A., and Gulla, G. 2015. "Weathering Grade in Granitoid Rocks: The San Giovanni in Fiore Area (Calabria, Italy)." *Journal of Maps*: 1-16.
- [24] Novotny, J. 2013. "Varnes landslide classification (1978)." Addis Ababa University, Ethiopia.
- [25] Balco, G., Stone, J. O., Lifton, N. A., and Dunai, T. J. 2008. "A Complete and Easily Accessible Means of Calculating Surface Exposure Age or Erosion Rate from ^{10}Be and ^{26}Al Measurements." *Quaternary Geochronology* 3: 174-95.
- [26] Schaller, M. et al. 2001. "Large-Scale Erosion from in Situ-Produced Cosmogenic Nuclides in European River Sediments." *Earth and Planetary Science Letter* 188: 441-58.